CHAPTER V

EXPERIMENTAL INVESTIGATION ON METHANE HYDRATE FORMATION KINETICS IN THE PRESENCE OF MIXED HYDRATE PROMOTERS FOR GAS STORAGE APPLICATION

5.1 Abstract

Gas hydrate is not only important for energy resources but also is of interest for the process to store and transport gas in the hydrate form. Two different promoters, tetrahydrofuran (THF) and sodium dodecyl sulfate (SDS), were investigated for methane hydrate formation kinetics. The concentrations were prepared at 1, 3, and 5.56 mol% for THF and 1, 4, and 8 mM for SDS. The experiments were conducted in a quiescent condition in a fixed volume crystallizer at 8 MPa and 4 °C. The results showed that all concentration of SDS and THF enhanced the methane hydrate formation kinetics and methane consumption compared to pure water, except 1 mol% of THF. In addition, the mixture of 1 mM SDS and 1 mol% THF showed the synergetic effects on the methane hydrate formation kinetics by forming the fastest methane hydrate due to SDS decreased the surface tension of water, and THF only enhanced the methane hydrate to form in structure II and more stable hydrate than pure water. The time required to achieve 90% of the final methane uptake (t_{90}) was employed to study the kinetic rate of methane hydrate formation. The 5.56 mol% THF/CH_4 system showed the fastest t_{90} at about 32.9 min. The average methane hydrate yields were also calculated in the range of 7.04 – 51.0 mol% in the experiments at 8 MPa and 4 °C.

Keywords: Methane; Hydrate; Formation; Tetrahydrofuran; Sodium dodecyl sulfate; Promoter

5.2 Introduction

Clathrate hydrates or gas hydrates are solid crystalline and non-stoichiometric compounds, in which gas guest molecules are trapped by hydrogen bond framework of the water lattice and stable at low temperature and high pressure (Sloan and Koh, 2008). Generally, gas hydrates are often found in the permafrost region or under the deep ocean. There are three well-known structures of gas hydrates, including sI, sII, and sH (Englezos, 1993; Sloan and Koh, 2008). Hence, the amount of gas, which can be stored in the hydrate form, depends on the available cages of the hydrate structures. The sI unit cell contains 46 water molecules and eight cages (two 12-hedra (5^{12}) and six 4-hedra ($5^{12}6^{12}$)), which can host small molecules like methane and carbon dioxide. The unit cell of sII consists of 136 water molecules and eight large cages ($5^{12}6^{4}$) and sixteen small cages (5^{12}); thus, larger gas guest molecules such as propane and isobutane can form the hydrate in this structure. The sH hydrate contains three different cages, three 5^{12}-cages, two $4^{3}5^{6}6^{3}$-cages, and one $5^{12}6^{8}$-cage (Sloan and Koh, 2008).

Methane gas is the most common gas guest molecule in natural gas hydrate (NGH). Although gas hydrates are concerned as the pipeline blockage in oil and gas industry (Chatti *et al.*, 2005; Panter *et al*, 2011; Koh *et al.*, 2011), it has been realized that natural gas hydrates are a great potential natural gas source of energy. Natural gas hydrates are not only important for the potential energy source but also considered as the method for gas storage and transportation due to its high capacity per unit volume (Kang and Lee, 2000; Sloan, 2003; Englezos and Lee, 2005; Linga *et al.*, 2007; Mandal and Laik, 2008; Li *et al.*, 2010; Koh *et al.*, 2011; Kim *et al.*, 2011; Veluswamy *et al.*, 2014a). For example, 170 m^3 of methane gas at STP can be stored in a unit volume of the hydrate (Englezos and Lee, 2005). The main issues of storing gas in the hydrate form are the slow kinetic rates of the hydrate formation and its stability. To store and transport natural gas in a hydrate form, the hydrate formation rates and the stability need to be improved. It has been reported that tetrahydrofuran (THF) can form the hydrate in the large cages of structure II (sII); therefore, the small cages are empty and could be occupied by methane gas (Kim *et al.*, 2006; Prasad *et al.*, 2009). Moreover, THF is defined as the thermodynamic promoter in the gas hydrate formation, which shifts the hydrate phase equilibrium and extends the stability zone of the hydrate (Susilo *et al.*, 2008; Strobel *et al.*, 2009; Chari *et al.*, 2012). Many experiments on the gas hydrate formation with the presence of THF focused on the thermodynamic data. Less information is available on the kinetics of gas hydrates formation. Previously, Florusse *et al.* (2004) added THF to increase the hydrogen hydrate formation at low pressure by reducing the formation pressure from 300 MPa at 27 °C to 5 MPa at 6.6 °C. Lee *et al.* (2005) reported that the molecule of THF occupied the large cages of sII, which reduced the hydrogen storage capacity in the hydrate. Linga *et al.* (2007) used THF as a promoter for carbon dioxide capture from a flue gas. They observed that THF decreased the rates and gas consumption. Chari *et al.* (2012) investigated the methane hydrate phase equilibrium of mixed hydrate with the presence of THF. They reported that, with the certain amount, the methane hydrate was formed in two structures, sI and sII. The methane hydrate phase equilibrium was also changed after adding THF. Veluswamy and Linga (2013) formed the hydrogen hydrate by adding THF as a promoter. The result indicated that the rate of hydrate growth increased at the high concentration of THF. Another work by Veluswamy *et al.* (2014b) compared the impact of THF, tetra-n-butylammonium bromide (TBAB), and cyclopentane (CP) as a hydrate promoter on hydrogen hydrate. The results indicated that the presence of THF showed the best performance on hydrogen uptake capacity; however, it was not stable compared to the other promoters.

Furthermore, an anionic surfactant such as sodium dodecyl sulfate (SDS) is described as a gas hydrate promoter, which decreases the surface tension of water and form micelles resulting in the hydrate formation rates. Ganji *et al.* (2007a, 2007b) investigated the effect of different surfactants on methane hydrate formation. They found that SDS exhibited the maximum promotion effect on the formation rate and the stability of the hydrate. The effects of SDS on ethane hydrate were studied by Mandal and Laik (2008). They demonstrated that the presence of SDS increased the gas consumption and storage capacity of ethane and also increased the dissociation rate. Partoon *et al.* (2013) studied the low-dosage of SDS on carbon dioxide hydrate formation. They reported that the small amount of SDS increased the induction time and gas consumption of carbon dioxide hydrate formation, but the gas consumption decreased when the concentration was higher than the CMC point. Hao *et al.* (2014) reported that using SDS was efficient to enhance the methane hydrate formation rate and the storage capacity. Veluswamy *et al.* (2015) also emphasized the effect of SDS by conducting the experiment on mixed hydrogen/propane hydrates. They reported that the presence of SDS reduced the induction time even with low SDS concentration. However, the final gas uptake performed with SDS was similar to the experiments conducted without surfactant.

In this study, these two hydrate promoters, THF and SDS, and their mixture were investigated for their effects on the methane hydrate formation kinetics in the static condition. Moreover, the induction time, time required to achieve 90% of the final methane uptake (t_{90}), methane consumption, and the storage capacity were reported.

5.3 Experimental

5.3.1 Materials and Apparatus

Ultra high purity methane (99.999 %, Labgaz Thailand Co., Ltd.), distilled deionized water, tetrahydrofuran (THF, 99.8 %, Lab-Scan, Thailand), sodium dodecyl sulfate (SDS, 99.0 %, Sigma-Aldrich) were used for hydrate formation. Figure 5.1a presents the schematic of the gas hydrate apparatus, consisting of a high-pressure stainless steel crystallizer (CR) with the internal volume of 50 mL and supply gas or a reservoir (R). The crystallizer and reservoir were immersed in a water bath, which controlled the temperature by an external refrigerator. Two pressure transmitters (Cole Parmer, model 68073-68074) with 0.13 % global error were used to measure the pressure. The temperature in the crystallizer was measured by four k-type thermocouples, located at different positions, as seen in Figure 5.1b: T1 at the top of the bed, T2 at the middle of the bed, T3 at the bottom of the bed, and T4 at the bottom of the crystallizer. A data logger (AI210, Wisco Industrial Instruments, Thailand) was connected to a computer to record the data during the experiment. All experiments were carried out in the quiescent condition with a fixed amount gas and water in the closed system.

5.3.2 Hydrate Formation Experiment

The concentrations of promoter solution were prepared at 1, 3, and 5.56 mol% for THF and 1, 4, and 8 mM for SDS. In order to investigate the effect of mixed hydrate promoters, SDS with the concentration of 1 mM was mixed with 1 mol% THF solution. Approximately, 30 mL of the solution was added into the crystallizer at each experiment. The crystallizer was pressurized to 0.5 MPa and depressurized to atmospheric pressure twice to eliminate the presence of air bubble in the system. The experimental condition is set at 8 MPa and 4 °C The data was then recorded every 10 s by the data logger. During the hydrate formation, the pressure in the crystallizer was decreased due to the gas consumption. The experiments continued until there was no further pressure drop at least 1 h. The pressure and temperature data were used to calculate the moles of methane consumed by equation 5.1;

$$\Delta n_{H,\downarrow} = n_{H,0} - n_{H,t} = \left(\frac{PV}{zRT}\right)_{\mathrm{G},0} - \left(\frac{PV}{zRT}\right)_{\mathrm{G},\mathrm{t}} \tag{5.1}$$

where $\Delta n_{H,\downarrow}$ is the number of moles of gas consumed for hydrate formation at the end of experiment. $n_{H,0}$ is the number of moles of hydrates at time zero. $n_{H,t}$ is the number of moles of the hydrates at time t. Subscripts of $G,0$ and G,t represent the gas phase at time zero and time t, respectively. P and T are the pressure and temperature in the system. V is the volume of gas phase in the crystallizer. R is the universal gas constant. z is the compressibility factor calculated by Pitzer's correlation (Babu *et al.*, 2013; Veluswamy and Linga, 2013).

In the THF solution, the conversion of water to hydrates was calculated with equation 5.2 (Veluswamy and Linga, 2013);

$$\text{Conversion (\%)} = \frac{\left(\Delta n_{H,\downarrow} + \Delta n_{THF}\right) \times \text{Hydration number}}{n_{H_2O}} \times 100 \tag{5.2}$$

where n_{H_2O} is the number of moles of water in the system. The hydration number is the number of water molecules per gas molecules to form the hydrate structure, 5.66 for the experiment conducted with THF and 5.75 for the experiment conducted without THF. Δn_{THF} is the number of moles of THF consumed for the hydrate formation at the end of experiment, which was calculated based on the assumption that THF occupied only the large cage of sII, as seen in equation 5.3 (Veluswamy and Linga, 2013);

$$\Delta n_{THF} = \Delta n_{H,\downarrow} \times \frac{\text{number of large cages}}{\text{number of small cages}} \tag{5.3}$$

The methane hydrate yield was measured by equation 6.4 in the closed system.

$$\text{Methane hydrate yield (mol\%)} = \frac{\text{Methane consumed (mol)}}{\text{Methane input (mol)}} \times 100 \tag{5.4}$$

5.4 Results and Discussions

5.4.1 Effect of Sodium Dodecyl Sulfate (SDS)

Figure 5.2 presents the typical methane uptake and temperature profiles of experiment conducted with the presence of 8 mM at 8 MPa and 4 °C. As seen from the figure, the methane uptake is suddenly increased at the initial stage as same as the temperature in the bulk liquid, detected by thermocouples inside the crystallizer due to the exothermic process of the hydrate formation. After that, the methane gas is consumed to grow the hydrate crystal until reaching the plateau, meaning that no more gas is allowed to form the hydrate with free water. Furthermore, the methane uptake is increased enormously again in the crystallizer, which is attributed to the hydrate formation in the bulk water. These results can be explained by the mechanism of methane hydrate formation with the presence of SDS. Yoslim *et al.* (2010) observed the mechanism of hydrate growth through a hollow polycarbonate (Lexan) column and demonstrated that with a thermocouple present at the surface of liquid phase, the hydrate crystal started to form at the surface of liquid, where the thermocouple was located and grew to cover all the gas-liquid interface. At the same time, the water level was decreased due to the water was delivered to grow the hydrate chunk. With less support from the bottom, the hydrate chunk would drop back to the bulk water and leave the wet surface of the wall that would quickly form the hydrate again. Contrarily, the crystallizer in this study was made from stainless steel; thus, the mechanism of hydrate growth is different. In other words, the methane hydrate could form as snowflakes (Kalogerakis *et al.*, 1993; Zhong and Rogers, 2000; Rogers *et al.*, 2007) or an open porous hydrate structure (Gayet *et al.*, 2005) suspended at the liquid interface. Meanwhile, the hydrate particles prefer to move to the crystallizer wall than thermocouples due to the conductive removal of the latent heats from the hydrate formation process by colder metal surface and grow upward along the wall (Kalogerakis *et al.*, 1993). Gayet *et al.* (2005) and Yoslim *et al.* (2008) stated that the capillary suction of the liquid from the bulk upward to the free wall can renew the gas-liquid interface of the hydrate growth front. It is believed that the hydrate particles are creeping along the wall of crystallizer until it blocks the gas inlet hole, located at the side of crystallizer (Figure 5.1b), showing in the first plateau in Figure 5.2. Later, the hydrate that blocks the gas inlet hole is cracked and the free gas is consumed to form the hydrate continuously until it reaches the equilibrium as shown by the second plateau in Figure 5.2.

To further clarify this behavior in this specific crystallizer, Figure 5.3 presents the methane hydrate sample in the experiment conducted with 8 mM SDS at 8 MPa and 4 °C. It can be seen from Figure 5.3a that the hollow hydrate sample is observed and the thermocouple tip is covered by hydrate particles, indicating that the methane hydrate is formed along the crystallizer wall. Figure 5.3b shows the blockage of gas inlet hole as pointed. Eventually, it can be noted that the crystallizer design in this study is not proper to conduct the experiment with the certain amount of surfactant due to the gas inlet hole blockage, causing the slow kinetic rates and low methane hydrate yield than it should be.

Figure 5.4 shows the typical methane uptake and temperature profiles of experiment conducted with different SDS concentrations. From the figure, the methane uptake profile of 1 mM SDS is distinctively difference from the others. In other words, it takes a longer time to form the hydrate, about 10 h, and only the first stage of gas uptake is observed. This indicates that the hydrate crystal maintains stable at the gas-water interface, while, in the experiment conducted with 4 mM and 8 mM, the second stage of hydrate growth is observed resulting in higher methane uptake, as discussed previously. It should be noted that a longer time of methane hydrate formation is not suitable for gas storage and transport applications.

Meanwhile, the 4 mM and 8 mM SDS exhibit almost the same gas uptake profile but the time for the first hydrate formation in 4 mM is longer than at 8 mM.

Table 5.1 shows the methane hydrate formation data of the experiments conducted with SDS at 8 MPa and 4 °C. As seen form the table, the experiment conducted with pure water (Exp. 1) does not show any evidence of hydrate formation during 48 h. This may be caused by 1) the hydrate could form a thin film on the interface of gas-solution, which then prevents the methane gas diffusion to the liquid phase for further hydrate growth (Erik *et al.*, 2001; Jiang *et al.*, 2008; Fandiño and Ruffine, 2014), and 2) The needle-like dendritic crystal could be formed at the interface of liquid phase and does not develop downward (Yoslim *et al.*, 2010); therefore, the form of hydrate cannot be observed in the experiment. It can be deduced from Table 5.1 that with the presence of SDS, the hydrate formation kinetics is enhanced compared to pure water. It is this gas hydrate formation rate that is considered as an important factor for gas storage and transport applications (Zhong and Rogers, 2000; Sun *et al.*, 2003; Lin *et al.*, 2004; Jiang *et al.*, 2008; Fandiño and Ruffine, 2014). The induction times listed in the table indicate the first hydrate formation in the experiments. It can be noted that the induction time of methane hydrate formation is decreased with the increase in the concentration of SDS due to the surface tension of the liquid phase is decreased, and a film-like interface is created along the wall. It is believed that this film is a preferred location for nucleation and initiation of gas hydrate (Yoslim *et al.*, 2008 and 2010).

To further investigation the kinetic effect of SDS, time required to achieve 90 % (t_{90}) of final gas uptake is present in Figure 5.5. It can be clearly seen that the average time is the shortest for the 1 mM SDS concentration at 17.0 min, followed by 172 and 205 min for 8 mM and 4 mM, respectively. Note that t_{90} is counted from the induction time (first hydrate formation). Although, the 1 mM SDS solution has the shortest t_{90}, it shows the longest induction time to form the first hydrate, and the methane hydrate yield is relatively low due to methane hydrate formation takes place only in the first stage of, as shown in Table 5.1. On the contrary, Veluswamy *et al.* (2015) demonstrated that t_{90} was higher for lower SDS concentration, but SDS had no effect on t_{90} at higher concentration. For the methane gas storage application, the methane yield is measured to quantify the effect of SDS concentration. It can be deduced that the average methane hydrate yield is increased with the increase of SDS concentration. The experiment conducted at 1 mM SDS concentration shows a low average methane hydrate yield due to the hydrate formation is stable in this condition and does not grow downward in the bulk water unlike at 4 mM and 8 mM. Moreover, the methane hydrate yields in the range of 5.02 – 52.5 % are achieved for any given SDS concentrations.

5.4.2 Effect of Tetrahydrofuran (THF)

Table 5.2 summarizes the data of methane hydrate formation with THF at 8 MPa and 4 °C. As seen from the table, the experiment conducted with water or 1 mol% THF at 8 MPa do not show the evidences of the hydrate formation after 48 h. In can be noted that the low concentration of THF does not affect the hydrate formation kinetics, while the hydrate formation kinetics is significantly influenced by the higher THF concentration. In addition, the experiments conducted with 3 and 5.56 mol% THF start to form the hydrate within 10 min. The induction time of experiment conducted with 5.56 mol% THF (theoretical concentration of THF hydrate formation) shows the average methane hydrate induction time at about 1.78 min, which is shorter than that with 3 mol% THF, as shown in the table. Moreover, the time required for 90 % of the final methane uptake with the presence of THF is also reported. As seen from Table 5.2, the system of 5.56 mol%THF/CH_4 shows a shorter time to reach 90 % of the final methane uptake than the system of 3 mol%THF/CH_4. This is because the methane hydrate phase equilibrium with the presence of THF is shifted to higher temperature and lower pressure than that of pure water (Susilo *et al.*, 2008; Strobel *et al.*, 2009; Chari *et al.*, 2012).

Although the system of 5.56 mol%THF/CH_4 exhibits a shorter time of the first hydrate formation and the time to achieve 90 % of the final methane uptake than the system of 3 mol%THF/CH_4, the methane consumption and methane hydrate yield shows otherwise. In other words, the average methane consumed and methane hydrate yield of the experiment conducted with 5.56 mol% THF is lower than with 3 mol% THF. These results may be caused by the fast methane hydrate formation at higher THF concentration on the gas-water interface that covered and blocked the gas molecules to grow the hydrate crystal, while at lower concentration of THF, the hydrate grows slowly and forms the hydrate crystals through the multiple nucleation of gas hydrate. This explanation corresponds to the methane uptake and temperature profiles of the experiments conducted with 3 and 5.56 mol% of THF as presented in Figure 5.6. It can be deduced from the figure that the experiment conducted with 3 mol% THF shows multiple methane hydrate formation after the first hydrate is formed, observed by the temperature profiles at different locations in the crystallizer and consumed more methane gas than the experiment conducted with 5.56 mol% THF, which is observed only the first stage of methane uptake.

Further explanation on these results can be attributed to the structures of methane hydrate formation, characterized by the ratio of structure I to structure II hydrates (sI/sII), as shown in Table II. The average ratio of sI/sII indicates how much hydrate formed in each structure. The calculation of sI or sII hydrates is based on the assumption that, with the presence of THF, gas hydrate should be fully occupied in the small cages of structure II due to the thermodynamics effect of THF before continue occupying the small cages and large cages of structure I. For instance, in the system of 5.56 mol% THF/CH_4, methane hydrate forms only in sII; therefore, the ratio is equal to 0. When the concentration of THF is decreased to 3 mol%, the ratio of sI/sII is changed, implying that the methane hydrate is formed in both structures. In this case, methane hydrate can be formed by the mole ratio of methane to water of 1:5.75 for structure I and 1:5.66 for structure II. That is the reason that the system of 3 mol% THF/CH_4 shows higher methane consumed and methane hydrate yield than that of 5.56 mol% THF/CH_4. These results are in agreement with Chari *et al.* (2012), who reported that the structure II of hydrate was observed when the mole fraction of THF was higher than 0.0556, and the structure I was no longer existed (Chari *et al.*, 2012; Sharma *et al.*, 2014). Furthermore, the average methane hydrate yield is 19.1 and 34.1 % in the experiments conducted with 5.56 and 3 mol% THF, respectively.

5.4.3 Effects of Mixed THF-SDS Promoters

The effect of mixed hydrate promoters is carried out in order to enhance the methane hydrate formation kinetic of 1 mol% THF/CH_4 system. In the case of no hydrate formation in the system of 1 mol% THF/CH_4, a small amount of SDS concentration of 1 mM is added to the mixture. The typical methane uptake and temperature profiles of the experiment conducted with 1 mM SDS and 1 mol% THF at 8 MPa 4 °C is shown in Figure 5.7. From the figure, the two-stage of methane hydrate formation is clearly seen as same as the experiment conducted with 4 mM and 8 mM of SDS concentrations. The methane hydrate forms very fast after introducing methane gas into the system and grows the hydrate crystal until reaching the plateau for the first stage of methane hydrate formation. The second stage of methane uptake may be caused by the same effect in the system of 4 mM and 8 mM. As discussed previously, the hydrate crystal is initially formed like snowflakes suspended in the liquid phase. The hydrate particles appear to attach each other covering the liquid interface and creeping to the crystallizer wall. At the same time, water in the liquid phase is delivered to grow the hydrate crystal along the crystallizer wall as high as the gas inlet hole (Kalogerakis *et al.*, 1993; Zhong and Rogers, 2000; Rogers *et al.*, 2007; Yoslim *et al.*, 2008; Gayet *et al.*, 2005). Later, the hydrate at the gas inlet hole is cracked, and then the free gas is consumed to grow the hydrate crystal again until it reaches the equilibrium.

The results of the induction time, methane consumption, methane hydrate yield, and the sI/sII ratio of the 1 mM SDS/1 mol% THF/CH_4 system are also presented in Table 5.2. It clearly demonstrates that the mixture of 1 mM SDS/1 mol% THF shows the synergetic effects on the methane hydrate formation kinetics compared to the experiment conducted with only 1 mM SDS or 1 mol% THF. The induction time of methane hydrate formation is about 0.39 min, which is lower than the experiments conducted with 3 and 5.56 mol% THF. However, the time required to achieve 90 % of the final methane uptake (t_{90}) is not significantly difference from the system of 3 mol% THF/CH_4, but higher than that of the 5.56 mol%THF/CH_4 system. The average methane hydrate yield at about 41.8 mol% is observed for the mixture of 1 mM SDS/1 mol% THF/CH_4. In addition, the average sI/sII ratio of the mixture of 1 mM SDS/1 mol% THF/CH_4 is about 3.51, indicating that methane hydrate is formed mostly in structure I. At the same time, the average ratio of sI/sII of the system of 3 mol% THF/CH_4 indicates the methane hydrate information mostly in structure II. It should be noted that, although the hydrate structure of the 3 mol% THF/CH_4 system and the mixture of 1 mM SDS/1 mol% THF/CH_4 is different, the methane hydrate yield is almost the same as seen in Table 5.2. It is believed that the mixture of 1 mM SDS/1 mol% THF/CH_4 shows the synergy effect to promote the hydrate formation and take up more methane gas as high as the system of 3 mol% THF/CH_4 regardless of the low concentration.

Consequently, the rate of methane hydrate formation can be deduced by the induction time and t_{90}. Figure 5.8 shows the effect of gas hydrate promoters on t_{90} for all experiments. As seen from the figure, the fastest time to reach 90% of methane uptake is found in the system of 1 mM SDS, but it takes the longest induction time in the range of 657 – 725 min and has the lowest methane hydrate yield. The 5.56 mol% THF/CH_4 system shows the thermodynamic effects on the methane hydrate formation rate with a shorter induction time and t_{90} than the others with the same promoter. It should be noted that THF promoter has significant effects on the methane hydrate formation rate more than SDS. Although the system of 5.56 mol% THF/CH_4 shows the faster rate of methane uptake than that with the mixture of THF-SDS indicated by t_{90}, the induction time has the opposite trend. This clearly demonstrates that the presence of 1 mM SDS and 1 mol% THF in pure water shows the synergy effects on the kinetic of methane hydrate formation. In other words, in the system of 1 mol% THF/CH_4, no hydrate formation is observed for 48 h; however, adding 1 mM SDS into 1 mol% THF solution can enhance the methane hydrate formation kinetics. A small amount of SDS decreases the surface tension of water, resulting in the increase in the solubility of methane gas in water, as the fastest induction time is observed in the mixture of 1 mM SDS/1 mol% THF (Ganji *et al.*, 2007a and 2007b). Though the induction time of the mixture of 1 mM SDS/1 mol% THF is very fast, the kinetics of the hydrate formation rate is slower than the system of 5.56 mol% THF/CH_4; nevertheless, the methane hydrate formation kinetics, observed by t_{90} is faster than the system conducted with SDS and 3 mol% THF.

Furthermore, the induction time and t_{90} are not only important for methane storage and transport applications but the methane hydrate yield is also considered as a value to enhance the methane storage in the hydrate form. The effect of gas hydrate promoters on the methane hydrate yield is presented in Figure 5.9. As seen form the figure, the system of 8 mM/CH_4 shows the highest average methane hydrate yield at about 50.2 mol% followed by the mixture of 1 mM SDS/1 mol% THF, and the lowest is in 1 mM SDS/CH_4 system. In addition, the methane hydrate yield in the range of 5.02 – 52.5 mol% is observed in all experiments. This result emphasizes the synergetic effect of mixed THF-SDS hydrate promoters in term of gas hydrate formation yield. As the result, it is reasonable to note that the mixture of 1 mM SDS/1 mol% THF can be considered as a medium to store methane gas in the formation of hydrate in a quiescent system, particularly to reduce the induction time and to increase the storage capacity. Although the methane hydrate yield is lower than that in the system of 8 mM SDS/CH_4, the induction time is faster than 8 mM SDS/CH_4 system. However, the data on hydrate dissociation is required for methane gas production after storing methane gas in the hydrate form for gas storage and transport applications.

5.5 Conclusions

The effects of hydrate promoters including tetrahydrofuran (THF) and sodium dodecyl sulfate (SDS) on methane hydrate formation kinetics were demonstrated. The results showed that all promoter concentrations showed the significant enhancement of methane hydrate formation rate and methane consumption compared to the pure water except only the 1 mol% THF, which did not form the methane hydrate until 48 h. It is noted that THF and SDS is the thermodynamic and kinetic promoter, respectively. The mixture of 1 mM SDS/1 mol% THF showed the synergetic effects on the methane hydrate formation kinetics by decreasing the surface tension of water, which reduced the induction time and enhanced the storage capacity. The time required to achieve 90 % of the final methane uptake (t_{90}) including the induction time was employed to study the kinetic rate of methane hydrate formation. The 5.56 mol% THF/CH_4 system showed the fastest t_{90} at about 32.9 min at 8 MPa and 4 °C. The average methane hydrate yields in the range of 7.04 – 51.0 mol% were obtained in the experiments at 8 MPa and 4 °C.

5.6 Acknowledgements

This work was supported by The Royal Golden Jubilee Ph.D. Program (2.P.CU/51/J.1), Thailand Research Fund; The Petroleum and Petrochemical College (PPC), Chulalongkorn University, Thailand; National Metal and Materials Technology Center (MTEC) (MT-B-53-CER-09-269-G), Thailand; Center of Excellence on Petrochemical and Materials Technology (PETROMAT), Thailand; UOP, A Honeywell Company, USA.

5.7 References

Babu, P., Yee, D., Linga, P., Palmer, A., Khoo, B.C., Tan, T.S., and Rangsunvigit, P. (2013) Morphology of methane hydrate formation in porous media. Energy Fuels, 27, 3364-3372.

Chari, V.D., Sharma, D.V.S.G.K., and Prasad, P.S.R. (2012) Methane hydrate phase stability with the lower mole fractions of tetrahydrofuran (THF) and *tert*-butylamine (*t*-BuNH2). Fluid Phase Equilibria, 315, 126-130.

Chatti, I., Delahaye, A., Fournaison, L., and Petitet, J.P. (2005) Benefits and drawbacks of clathrate hydrates: a review of their areas of interest. Energy Conversion and Management, 46, 1333-1343.

Englezos, P. (1993) Clathrate hydrates. International Journal of Energy Research, 32, 1251-1274.

Englezos, P. and Lee, J.D. (2005) Gas hydrates - a cleaner source of energy and opportunity for innovative technologies. Korean Journal of Chemical Engineering, 22, 671-681.

Erik, M., Selim, M.S., and Sloan Jr., E.D. (2001) Methane hydrate film growth kinetics, Fluid Phase Equilibria, 185, 65-75.

Fandiño, O. and Ruffine, L. (2014) Methane hydrate nucleation and growth from the bulk phase: Further insights into their mechanisms. Fuel, 117, 442-449.

Florusse, L.J., Peters, C.J., Schoonman, J., Hester, K.C., Koh, C.A., Dec, S.F., Marsh, K.N., and Sloan, M.E. (2004) Stable low-pressure hydrogen clusters stored in a binary clathrate hydrate. Science, 30, 469-471.

Ganji, H., Manteghian, M., and Mofrad, H.R. (2007a) Effect of mixed compounds on methane hydrate formation and dissociation rates and storage capacity. Fuel Processing Technology, 88, 891-895.

Ganji, H., Manteghian, M., Zadeh, K.S., Omidkhah, M.R., and Mofrad, H.R. (2007b) Effect of different surfactants on methane hydrate formation rate, stability and storage capacity. Fuel, 86, 434-441.

Gayet, P., Dicharry, C., Marion, G., Graciaa, A., Lachaise, J., and Nesterov A. (2005) Experimental determination of methane hydrate dissociation curve up to 55 MPa by using a small amount of surfactant as hydrate promoter. Chemical Engineering Science, 60, 5751-5758.

Hao, S.Q., Kim, S., Qin, Y., and Fu, X.H. (2014) Enhanced methane storage using sodium dodecyl sulfate and coal. Environmental Chemistry Letters, 12, 341-346.

Jiang, G., Tu, Y., Ning, F., Zhang, L., Dou, B., and Wu, X. (2008, July 6-10) Effect of SDS and THF on formation of methane-containing hydrates in pure water. Paper presented at The 6th International Conference on Gas hydrates (ICGH 2008), Vancouver, Canada.

Kalogerakis, N., Jamaluddin, A.K.M., Dholabhai, P.D., and Bishnoi, P.R. (1993, March 2-5) Effect of surfactant on hydrate formation kinetics. Paper presented at SPE International Symposium on Oilfield Chemistry, New Orleans, Los Angeles, U.S.A.

Kang, S.P. and Lee, H. (2000) Recovery of CO_2 from flue gas using gas hydrate: Thermodynamic verification through phase equilibrium measurements. Environmental Science & Technology, 34, 4397-4400.

Kim, D.Y., Park, J., Lee, J.W., Ripmeester, J.A., and Lee, H. (2006) Critical guest concentration and complete tuning pattern appearing in the binary clathrate hydrates. Journal of the American Chemical Society, 128, 15360-15361.

Kim, N.J., Park, S.S., Kim, H.T., and Chun, W.A. (2011) Comparative study on enhanced formation of methane hydrate using CM-95 and CM-100 MWCNTs. International Communications in Heat and Mass Transfer, 38, 31-36.

Koh, C.A., Sloan, E.D., Sum, A.K., and Wu, D.T. (2011) Fundamental and applications of gas hydrates. Annual Review of Chemical and Biomolecular Engineering, 2, 237-257.

Lee, H., Lee, J.W., Kim, D.Y., Park, J., Seo, Y.T., Zeng, H., Moudrakovski, I.L., Ratcliffe, C.I., and Ripmeester, J.A. (2005) Clathrate hydrates for hydrogen storage. Nature, 434, 743-746.

Li, X.S., Xu, C.G., Chen, Z.Y., and Wu, H. (2010) Tetra-n-butyl ammonium bromide semi-clathrate hydrate process for post-combustion capture of carbon dioxide in the presence of dodecyl trimethyl ammonium chloride. Energy, 35, 3902-3908.

Lin, W., Chen, G.L., Sun, C.Y., Guo, X.Q., Wu, Z.K., Liang, M.Y., Chen, L.T., and Yang, L.Y. (2004) Effect of surfactant on the formation and dissociation kinetic behavior of methane hydrate. Chemical Engineering Science, 59, 4449-4455.

Linga, P., Adeyemo, A., and Englezos, P. (2007) Medium-pressure clathrate hydrate/membrane hybrid process for postcombustion capture of carbon dioxide. Environmental Science & Technology, 42, 315-320.

Linga, P., Daraboina, N., Ripmeester, J.A., and Englezos, P. (2012) Enhanced rate of gas hydrate formation in a fixed bed column filled with sand compared to a stirred vessel. Chemical Engineering Science, 68, 617-623.

Mandal, A. and Laik, S. (2008) Effect of the promoter on gas hydrate formation and dissociation. Energy Fuels, 22, 2527-2532.

Panter, J.L., Ballard, A.L., Sum, A.K., Sloan, E.D., and Koh, C.A. (2011) Hydrate plug dissociation via nitrogen purge: experiments and Modeling. Energy Fuels, 25, 2572-2578.

Partoon, B., Malik, S.N.A., Azemi, M.H., and Sabil, K.M. (2013) Experimental investigations on the potential of SDS as low-dosage promoter for carbon dioxide hydrate formation. Asia-Pacific Journal of Chemical Engineering, 8, 916-921.

Prasad, P.S.R., Sowjanya, Y., and Prasad, K.S. (2009) Micro-raman investigations of mixed gas hydrates. Vibrational Spectroscopy, 50, 319-323.

Rogers, R., Zhang, G., Dearman, J., and Woods, C. (2007) Investigations into surfactant/gas hydrate relationship. Journal of Petroleum Science and Engineering, 56, 82-8.

Sharma, D.V.S.G.K., Sowjanya, Y., Chari, V.D., Prasad, P.S.R., Methane storage in mixed hydrates with tetrahydrofuran. Indian Journal of Chemical Technology, 21, 114-119.

Sloan, E. D. (2003) Fundamental principles and applications of natural gas hydrates. Nature, 426, 353-359.

Sloan, E.D. and Koh, C.A. (2008) Clathrate Hydrates of Natural Gases, 3rd ed., New York: CRC Press.

Strobel, T.A., Koh, C.A., and Sloan, E.D. (2009) Thermodynamic predictions of various tetrahydrofuran and hydrogen clathrate hydrates. Fluid Phase Equilibria, 280, 61-67.

Sun, Z., Wang, R., Ma, R., Guo, K., and Fan, S. (2003) Effect of surfactants and liquid hydrocarbons on gas hydrate formation rate and storage capacity. International Journal of Energy Research, 27, 747-756.

Susilo, R., Alavi, S., Ripmeester, J.A., and Englezos, P. (2008) Tuning methane content in gas hydrates via thermodynamic modeling and molecular dynamics simulation. Fluid Phase Equilibria, 263, 6-17.

Veluswamy, H.P., Chen, J.Y., and Linga, P. (2015) Surfactant effect on the kinetics of mixed hydrogen/propane hydrate formation for hydrogen storage as clathrates. Chemical Engineering Science, 126, 488-499.

Veluswamy, H.P., Chin, W.I., and Linga, P. (2014) Clathrate hydrates for hydrogen storage: The impact of tetrahydrofuran, tetra-n- butylammonium bromide and cyclopentane as promoters on the macroscopic kinetics. International Journal of Hydrogen Energy, 39, 16234-16243.

Veluswamy, H.P., Kumar, R., and Linga, P. (2014) Hydrogen storage in clathrate hydrates: Current state of the art and future directions. Applied Energy, 122, 112-132.

Veluswamy, H.P. and Linga, P. (2013) Macroscopic kinetics of hydrate formation of mixed hydrates of hydrogen/tetrahydrofuran for hydrogen storage. International Journal of Hydrogen Energy, 38, 4587-4596.

Yoslim, J. and Englezos P. (2008, July 6-10) The effect of surfactant on the morphology of methane/propane clathrate hydrate crystals. Paper presented at The 6th International Conference on Gas hydrates, Vancouver, Canada.

Yoslim, J., Linga, P., and Englezos, P. (2010) Enhanced growth of methane–propane clathrate hydrate crystals with sodium dodecyl sulfate, sodium tetradecyl sulfate, and sodium hexadecyl sulfate surfactants. Journal of Crystal Growth, 313, 68-80.

Zhong, Y. and Rogers, E. (2000) Surfactant effects on gas hydrate formation. Chemical Engineering Science, 55, 4175-4187.

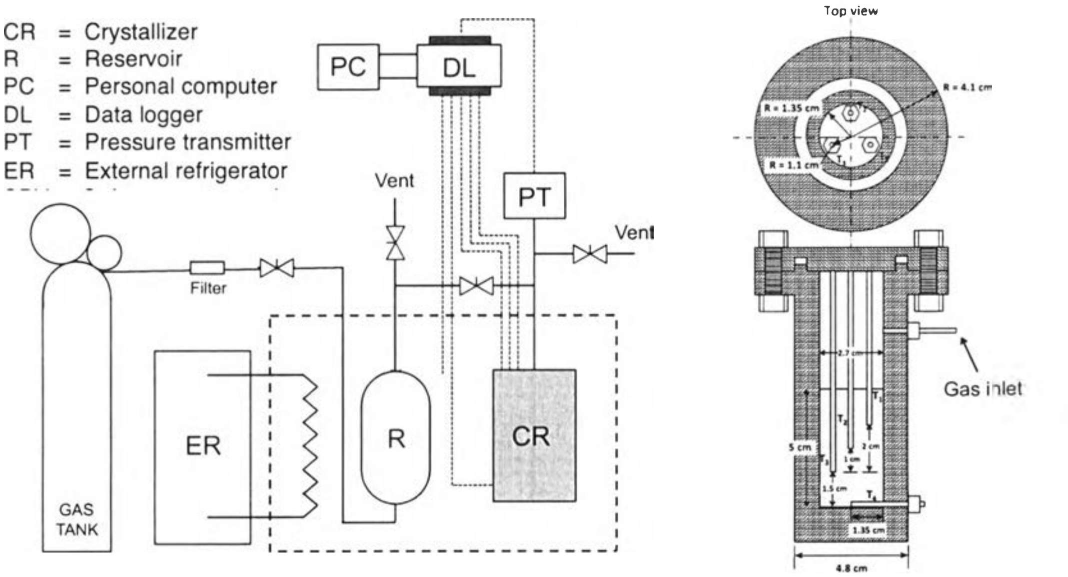

(a) (b)

Figure 5.1 Schematic diagram of gas hydrate apparatus: a) schematic diagram, b) cross-section of the crystallizer.

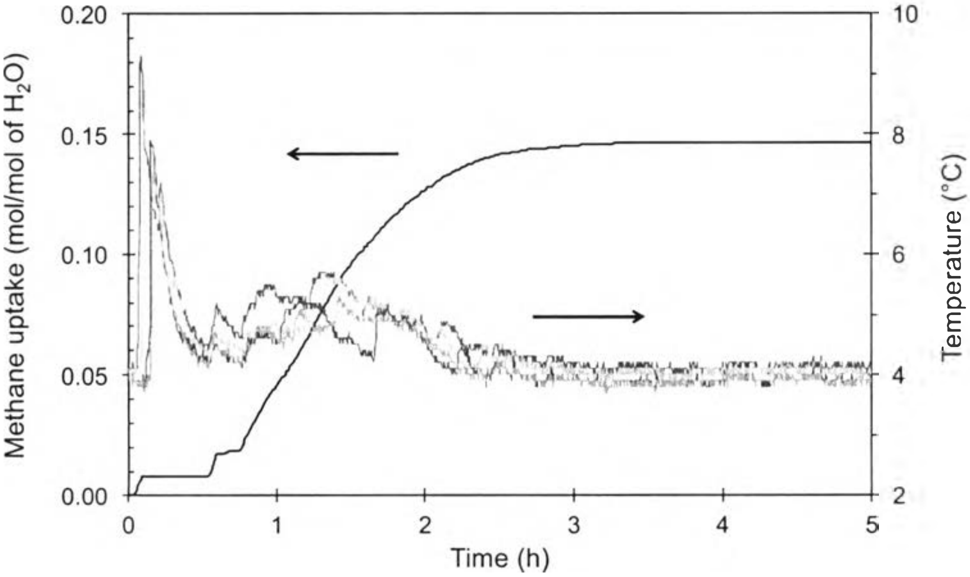

Figure 5.2 Typical methane uptake and temperature profiles of experiment conducted with the presence of 8 mM at 8 MPa and 4 °C (Exp. 8, Table 5.1).

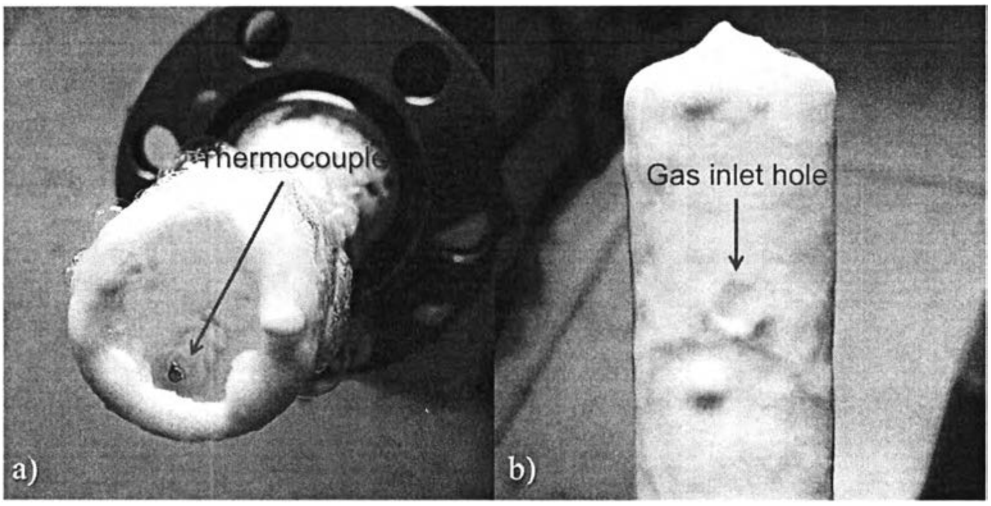

Figure 5.3 Methane hydrate samples in the experiment conducted with 8 mM SDS at 8 MPa and 4 °C.

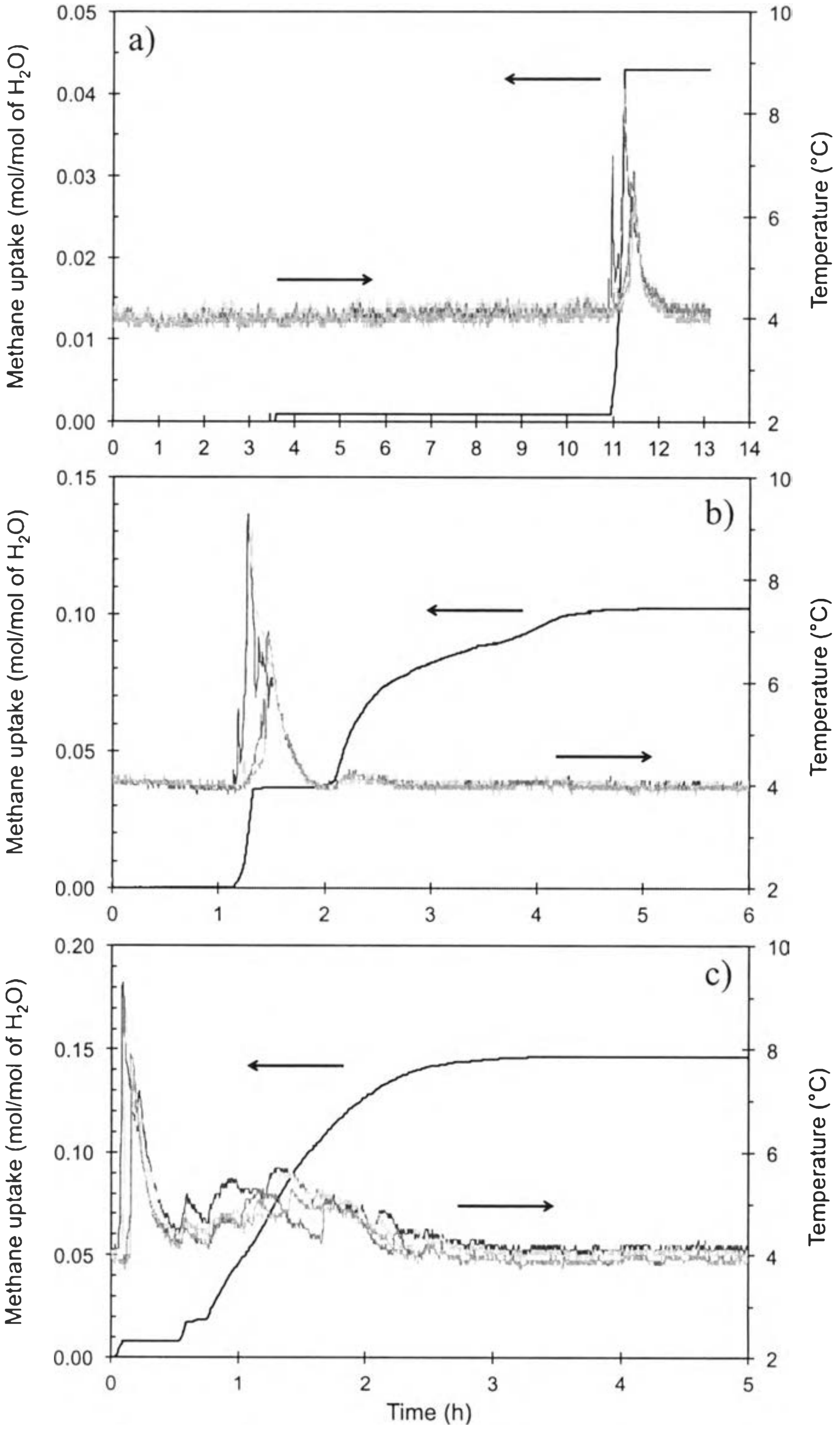

Figure 5.4 Typical methane uptake and temperature profiles of a) 1 mM SDS (Exp. 3, Table 5.1), b) 4 mM SDS (Exp. 6, Table 5.1), c) 8 mM SDS (Exp. 8, Table 5.1) at 8 MPa and 4 °C.

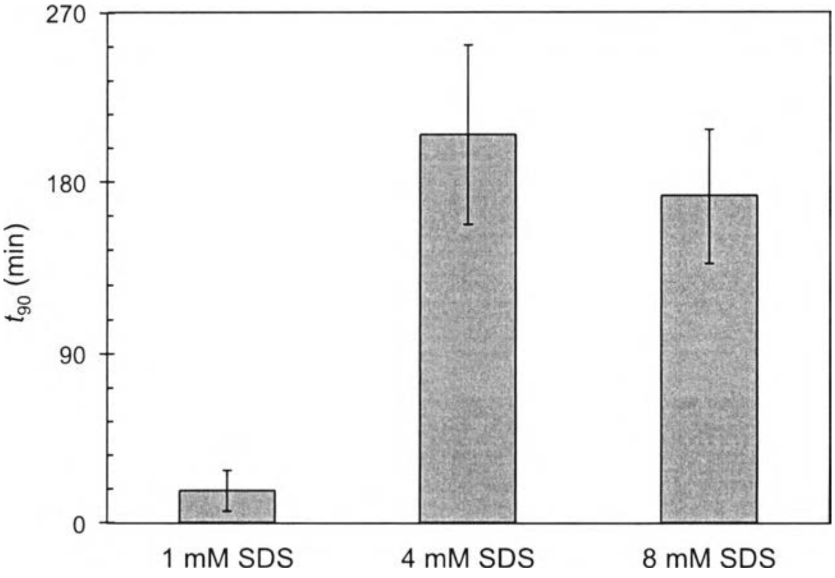

Figure 5.5 Effect of SDS concentration on t_{90} of the final methane uptake excluding the induction time.

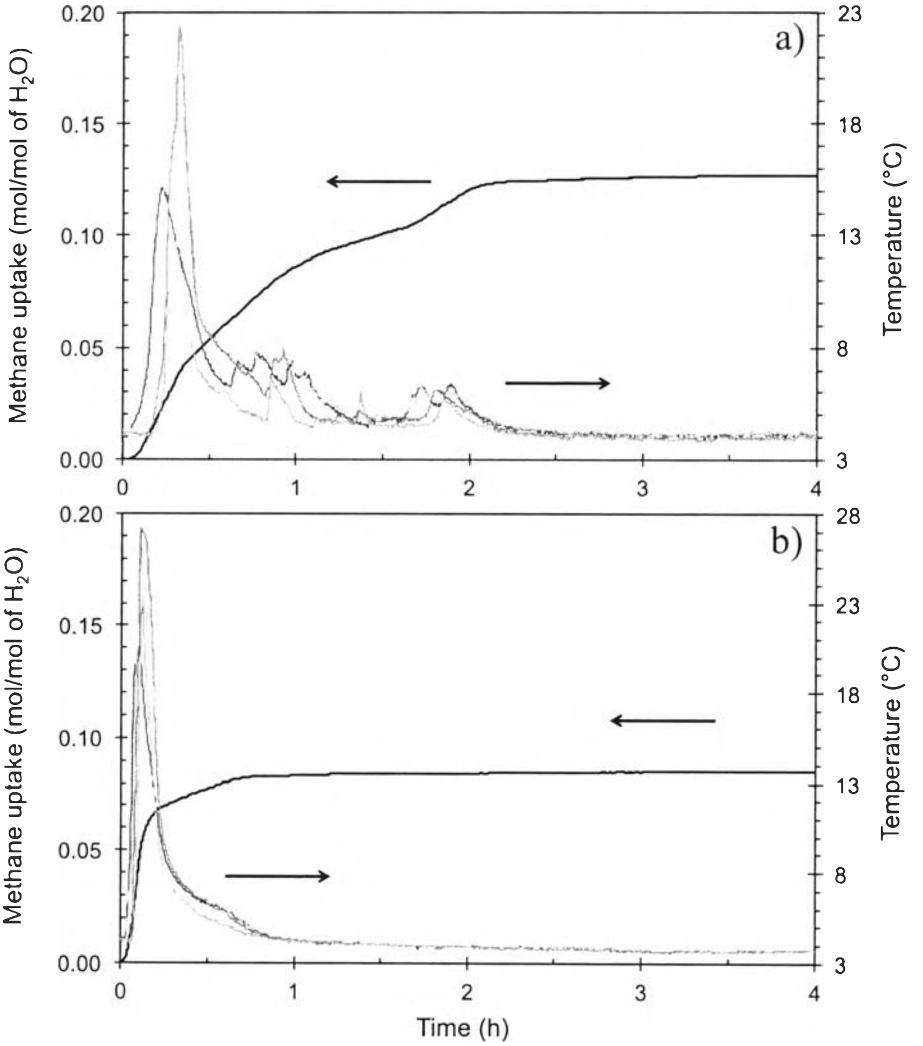

Figure 5.6 Typical methane uptake and temperature profiles of the experiment conducted with; a) 3 mol%THF (Exp. 2, Table 5.2) and b) 5.56 mol%THF (Exp. 7, Table 5.2) at 8 MPa and 4 °C.

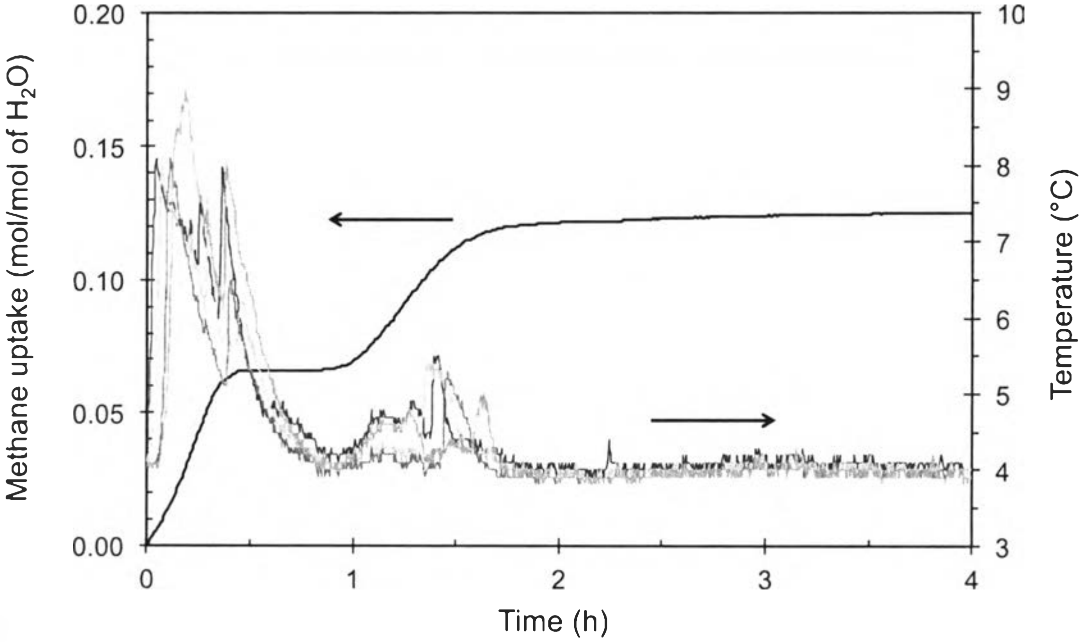

Figure 5.7 Typical methane uptake and temperature profiles of the experiment conducted with 1 mM SDS and 1 mol% THF at 8 MPa and 4 °C (Exp.10, Table 5.2).

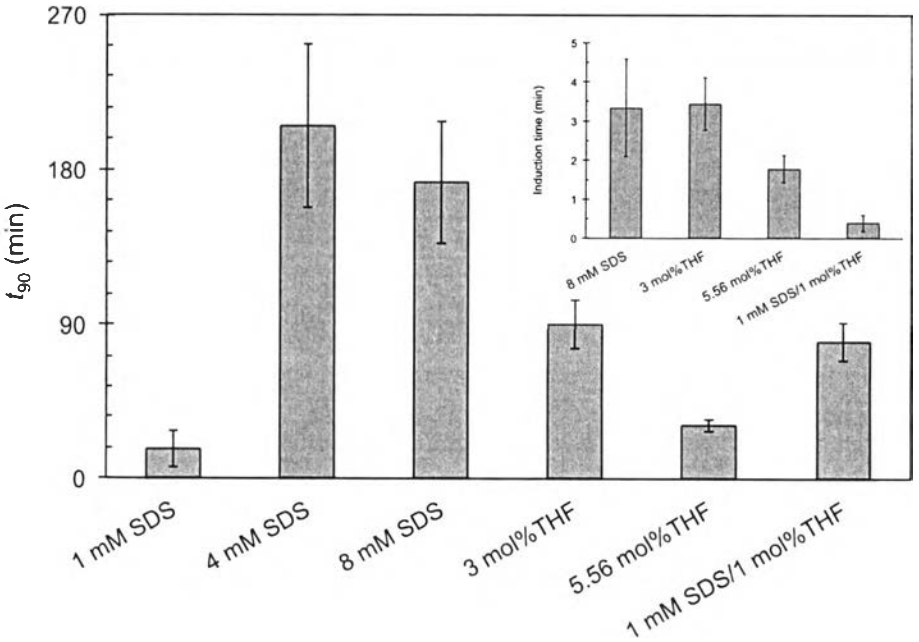

Figure 5.8 Effect of gas hydrate promoter on t_{90} of the final methane uptake excluding induction time for all experiments.

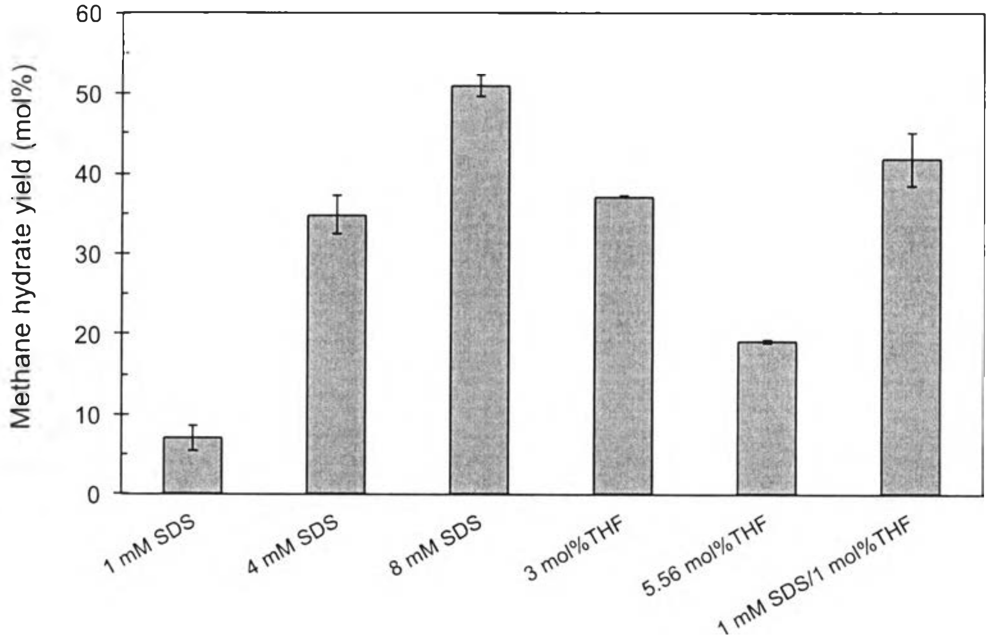

Figure 5.9 Effect of gas hydrate promoters on methane hydrate yield for all experiments.

Table 5.1 Methane hydrate formation experimental conditions of SDS at 8 MPa and 4 °C

Exp.	Induction Time* (min)	End of Experiment		
		Methane Consumed (mol/mol of H_2O)	t_{90}** (min)	Methane Hydrate Yield (mol%)
Pure water/CH_4				
1	DNF	-	-	-
1 mM SDS/CH_4				
3	657	0.0429	17	8.81
4	725	0.0427	30	7.29
5	712	0.0244	4	5.02
Avg.	**698±29.47**	**0.0367±0.0087**	**17.0±10.61**	**7.04±1.557**
4 mM SDS/CH_4				
6	70.8	0.1016	156	35.8
7	15.7	0.1014	253	33.8
8	65.7	0.1169	153	39.2
Avg.	**43.2±25.4**	**0.1015±0.0077**	**205±47.50**	**34.8±2.347**
8 mM SDS/CH_4				
8	3.67	0.1462	122	49.1
9	4.67	0.1529	199	51.3
10	1.67	0.1568	196	52.5
Avg.	**3.34±1.25**	**0.1520±0.0044**	**173±35.54**	**51.0±1.41**

DNF = no hydrate formation for 48 h.

*Induction time is the time it takes for the first hydrate formation.

** Time required to for the 90 % of the final gas uptake excluding the induction time.

Table 5.2 Methane hydrate formation experimental conditions with THF at 8 MPa and 4 °C

Exp.	Induction Time* (min)	End of Experiment			
		Methane Consumed (mol/mol of H_2O)	t_{90}** (min)	Methane Hydrate Yield (mol%)	sI/sII
		1 mol% THF/CH_4			
1	DNF	-	-	-	-
		3 mol% THF/CH_4			
2	3.83	0.1286	109	37.3	0.58
3	4.00	0.1273	76.5	37.0	0.57
4	2.50	0.1276	85.0	37.0	0.57
Avg.	**3.44±0.6706**	**0.1278±0.0006**	**90.2±13.83**	**37.1±0.1414**	**0.57±0.0**
		5.56 mol% THF/CH_4			
5	1.83	0.0759	33.5	18.9	0
6	1.33	0.0771	33.9	19.4	0
7	2.17	0.0763	26.1	19.1	0
Avg.	**1.78±0.3450**	**0.0764±0.0005**	**31.2±3.558**	**19.1±0.2055**	**0**
		1 mM SDS/1 mol% THF/CH_4			
8	0.67	0.1205	84.3	38.9	3.21
9	0.17	0.1425	65.3	46.4	3.93
10	0.33	0.1258	90.9	40.0	3.39
Avg.	**0.39±0.2085**	**0.1296±0.0094**	**80.2±10.83**	**41.8±3.3068**	**3.51±0.3**

DNF = no hydrate formation for 48 h.

*Induction time is the time it takes for the first hydrate formation.

** Time required to for the 90 % of the final gas uptake excluding the induction time.